Металлофиз. новейшие технол. / Metallofiz. Noveishie Tekhnol.
2015, т. 37, № 6, сс. 839–852
Оттиски доступны непосредственно от издателя
Фотокопирование разрешено только
в соответствии с лицензией

PACS numbers: 06.60.Vz, 42.62.Cf, 62.20.me, 62.20.mm, 81.20.Vj, 81.40.Np, 81.70.Bt

The Fatigue Strength of AISI 430–304 Stainless Steels Welded by CO_2 Laser Beam Welding

U. Caligulu, M. Turkmen*, A. Ozer**, M. Taskin, and M. Ozer***

Firat University, Faculty of Technology,
Department of Met. and Materials Eng.,
23119 Elazig, Turkey
**Kocaeli University,*
Hereke Vocational School,
41800 Kocaeli, Turkey
***Gazi University Technical Sciences Vocational School,*
Ostim Yenimahelle, Ankara, Turkey
****Gazi University, Technology Faculty,*
Department of Met. and Materials Eng.,
06500 Besevler, Ankara, Turkey

In this study, the fatigue strength of AISI 430–304 stainless steels welded by CO_2 laser beam welding (LBW) is investigated. Laser welding experiments are carried under helium atmosphere at 2000, 2250 and 2500 W welding powers with 100 cm/min welding speed. The welding zones are examined by optical microscopy, scanning electron microscopy, and energy dispersive spectroscopy analysis. Fatigue tests are performed using an axial fatigue test machine, and the fatigue strength is analysed drawing S–N curves and critically observing fatigue fracture surfaces of the tested samples. The experimental results indicate that mechanical properties and microstructural features are affected significantly by welding power. The fatigue strength of CO_2 laser welded samples increase due to higher deep penetration in welding zone with increasing welding power in chosen conditions. The best properties are observed with the specimens welded at 2500 W heat input and 100 cm/min welding speed.

В цій роботі досліджено втомну міцність неіржавійних сталей AISI 430–304, зварених променем CO_2-лазера. Експерименти з лазерного зварювання виконувалися в атмосфері гелію за потужности зварювання у 2000, 2250 і 2500 Вт із швидкістю зварювання у 100 см/хв. Зони зварювання досліджувалися методами оптичної мікроскопії, сканівної електронної мікроскопії та енергодисперсійної спектроскопії. Дослідження на втому виконувалися з використанням машини для випробувань на вісну втому, а втомна міцність аналізувалася шляхом побудови S–N-кривих та крити-

чного спостереження поверхонь втомного руйнування досліджених зразків. Експериментальні результати показують, що механічні властивості та мікроструктурні особливості значно залежать від потужности зварювання. Втомна міцність зразків, зварених CO_2-лазером, зростає завдяки збільшенню глибини проникнення в зоні зварювання зі збільшенням потужности зварювання за обраних умов. Найкращі властивості спостерігалися у зразків, зварених за підведеної теплоти при 2500 Вт та швидкости зварювання у 100 см/хв.

В данной работе исследована усталостная прочность нержавеющих сталей AISI 430–304, сваренных лучом CO_2-лазера. Эксперименты по лазерной сварке выполнялись в атмосфере гелия при мощностях сварки 2000, 2250 и 2500 Вт и скорости сварки 100 см/мин. Зоны сварки исследовались методами оптической микроскопии, сканирующей электронной микроскопии и энергодисперсионной спектроскопии. Испытания на усталость производились с использованием машины для испытаний на осевую усталость, а усталостная прочность анализировалась путём построения S–N-кривых и критического наблюдения поверхностей усталостного разрушения исследованных образцов. Экспериментальные результаты показывают, что механические свойства и микроструктурные особенности значительно зависят от мощности сварки. Усталостная прочность образцов, сваренных CO_2-лазером, возрастает благодаря увеличению глубины проникновения в зоне сварки с увеличением мощности сварки при выбранных условиях. Наилучшие свойства наблюдались у образцов, сваренных при подводимой теплоте с 2500 Вт и скорости сварки 100 см/мин.

Key words: fatigue strength, welding zone, stainless steels, AISI 430, AISI 304, CO_2 LBW.

(Received December 2, 2014; in final version, April 16, 2015)

1. INTRODUCTION

Stainless steels are iron-base alloys containing 8–25% nickel and more chromium than the 12% necessary to produce passivity but less than 30%. The steels resist both corrosion and high temperature. Stainless steels can be divided into five types as ferritic, austenitic, martensitic, duplex, and precipitation-hardening. Ferritic stainless steels are widely used due to the fact that their corrosion resistance is higher at room temperature and they are much cheaper than the other stainless steels. Ferritic stainless steels contain 16–30% Cr within their structures in respect of addition of the alloy element. This type of the steel can be shaped easily and resist atmospheric corrosion well and thanks to these characteristics, it has a wide range of application in architecture, interior and exterior decoration, kitchen utensils, manufacturing of wash boilers and drying machines, food industry, automotive industry, and petrochemical and chemical industries [1–4].

Austenitic-stainless steel is preferred more than other stainless-steel types due to easiness in welding process. Then, some negative metallurgic changes are taken into consideration in welding of the steels. These are the following ones: delta ferrite phase, sigma phase, stress-corrosion cracking, and chrome–carbide precipitate between grain boundaries at 450–850°C of Cr–Ni austenitic steels such as 18/8 joined by fusion welding in long waiting time. Stainless steels can generally be welded with all methods of fusion welding and solid state welding. Out of the fusion welding methods, electric arc welding, submerged arc welding, MIG, TIG, plasma welding, electron beam welding, resistance welding, and laser welding, *etc*. are widely used. In the fusion welding methods for joining stainless steel, brittle intermetallic compounds phases are produced in the fusion zone, which reduce the strength of the welding joint. However, in the LBW joining of stainless steel, because these phases are reduced, it improves the performance of the stainless steel joint [5–10].

Laser beam welding, using laser beam of high energy density as a heat source, is a highly efficient and precise welding method. It has some excellences, such as high energy density, focalization, deep penetration, high efficiency and strong applicability, and it is widely applied to welding zone requiring the high precision and high quality, including aviation and space flights, automobile, microelectronics, light industry, medical treatment and nuclear industry. As laser beam welding is a fast but unbalanced heat-circulation process, larger temperature degrees appear around the weld, therefore the residual stress and deformation of different extent can also appear in the post welding structure. All of these phenomena become important factors, influencing the quality of welding structure and the usable capability. Understanding the thermal process of welding is crucial to analyse the mechanical welding structure and microstructure as well as controlling of welding quality [11–14].

Fatigue is progressive localized permanent structural change that occurs in a material subjected to repeated or fluctuating strains at stresses having a maximum value less than the tensile strength of the material. It has been estimated that 90% of the failures, which occur in engineering components, can be attributed to fatigue and high portion of the fatigue failures are associated with a weldment with stress concentrations and possible weld defects [15]. Fatigue affecting factors are the following: material type, the effects of composition and structure, the effects of surface properties, the effect of the notch, the effects of strains, the effect of the corrosion, the effect of the working environment, construction and montage errors, the effect of temperature, the effect of frequency (test speed), and dimensional factors. Stresses, to be applied to parts during operation, may be different in type and severity. Depending on the type of stress, there are four main

types of fatigue test species. They are axial, bending, torsion and compound fatigue tests. Fatigue, crack initiation, crack propagation and breakage occur in three stages. Fatigue does not cause a significant plastic deformation of the material. Fatigue cracks occur in such places, where stress concentration, sharp edges, scratches, nicks and corrosion and fatigue move at certain speeds and cause the failure of material. Therefore, the design of parts working under dynamic loads should avoid sharp edges, which cause stress concentration and notches. In addition, the polished surfaces of components exposed to cyclic loading can extend fatigue life [16–18].

In order to optimize welding conditions for materials with different properties or advanced materials, experimental investigations are still required. Along with a great deal of researches devoted to the weldability of dissimilar materials and properties estimation for welding process, the further investigation on practical applications of failure is also becoming considerably important and urgent. It is well known that the majority of failures that occur in the structures are caused by fatigue failure in weldments due to fatigue type of loading experienced by the structures [19]. Very few studies have been carried out to evaluate the fatigue properties of AISI 430 ferritic stainless steel weld [20]. The fatigue process and its mechanism are largely influenced by the presence of material non-homogeneities. It has been found by several researchers that generally fatigue cracks originate either in the heat affected zone or in the weld materials due to fatigue loading and could be the potential source of catastrophic failures in some unfortunate situations [21].

Curcio *et al.* [22] analysed the parameters of various materials at laser welding and reported that welding power, welding speed, shielding gas, gas nozzle, and the process of focusing were among these parameters. Zambon *et al.* [23] analysed the microstructure and tensile stages of AISI 904L super austenitic stainless steel during CO_2 laser welding and reported that there was a decrease in flow resistance and detach tensile and depending on this there was an increase in hardness value because of rapid cooling of the fusion zone during welding. Bertrand *et al.* [24] analysed the Nd:YAG laser welding parameters of the stainless steel and reported that laser power was 600–2700 W and the welding speed was 3–10 m/min and flow speed of the shielding gas was similar to the surface contamination or it changed depending on various surface tensions. El-Batahgy [25] analysed the effects of austenitic stainless steels on surface of hardness and fusion zone of laser welding parameters and reported that penetration increased depending on the increased welding power and welding speed, there was not a significant difference between helium and argon shielding gases, and mechanical features (tension, hardness, bending) and fusion zone were not affected by heat input at room temperature. Ghani *et al.* [26] analysed the

microstructural characteristics of low carbon steels on Nd:YAG laser welding and reported that depending on the increased energy input and process speed, the hardness value of the material at welding zone also increased. Vural *et al.* [27] analysed the effect of welding nugget diameter on the fatigue strength of the resistance spot welded joints of different steel sheets and reported that galvanized steel sheet combination has the highest fatigue limit and crack growth rate of the spot welded galvanized AISI 304 joining type is slower than that of base metals given in literature. C and m coefficients of Paris–Erdogan equation for spot welded AISI 304 galvanized steel sheet joints were obtained. Yuri *et al.* [28] analysed the effect of welding structure on high-cycle and low cycle fatigue properties for MIG welded A5083 aluminium alloys at cryogenic temperatures and reported that in the high-cycle fatigue tests the ratios of 10^6 fatigue strength to tensile strength for A5183 weld metals were slightly lower than A5083, in the low-cycle fatigue tests fatigue lives for A5183 weld metals were slightly shorter than those for A5083. Jang *et al.* [29] analysed the effects of microstructure and residual stress on fatigue crack growth of stainless steel narrow gap welds and reported that the fatigue crack growth rate depended on both dendrite alignment and residual stress distribution in the weld, so the fatigue crack growth rates were the highest near the boundary between the inner weld deposit and the outer weld deposit, where the dendrites were well aligned and the high tensile residual stress existed. Taban *et al.* [30] analysed the laser welding of modified 12% Cr stainless steel, regarding strength, fatigue, toughness, microstructure, and corrosion properties, and reported that fatigue behaviour of clean 1.4003 ferritic stainless steel weld is excellent provided weld defects are omitted and all excess of weld metal is removed appropriately or at least the transition from weld to base metal is suitably smoothened. Under these conditions, the fatigue strength of butt welds is comparable with that of the base metal. The major withdrawal of the stainless steel is the tendency to grain coarsening at the HTHAZ.

In this study, the fatigue strength of AISI 430–304 stainless steels welded by CO_2 laser beam welding is investigated.

2. EXPERIMENTAL

AISI 430 steels comprise approximately one-half of the SAE-AISI type 400 series stainless steels. They are known with their excellent stress corrosion cracking resistance and good resistance to pitting and crevice corrosion in chlorine environments. Welding is known to reduce toughness, ductility and corrosion resistance because of the grain coarsening and carbide precipitations. The grain size gradually increases from the edge of Heat Effected Zone (HAZ) to the fusion boundary. Welding of 400 series usually requires preheat and post-

weld heat treatment to minimize stress that can lead to cracking [31]. AISI 304 steels comprise approximately one-half of the SAE-AISI type 300 series stainless steels. They are known with their excellent stress corrosion cracking resistance and good resistance to pitting and crevice corrosion in chlorine environments. Austenitic-stainless steel is preferred more than other stainless-steel types due to easiness in welding process. Then, some negative metallurgic changes are taken into consideration in welding of the steels. These are delta ferrite phase, sigma phase, stress-corrosion cracking, chrome-carbide precipitate between grain boundaries at 450–850°C of Cr–Ni austenitic steels such as 18/8 joined by fusion welding in long waiting time. Welding of 300 series usually requires preheat and post-weld heat treatment to minimize stress that can lead to cracking [32, 33]. The chemical compositions, mechanical properties and physical properties of both steels are given in Tables 1, 2, and 3, respectively.

Steel plates to be joined were cut at 45×90×4 mm^3 dimensions. 45 mm width is selected to achieve the standard length of 90 mm fatigue

TABLE 1. Chemical composition of AISI 430 ferritic stainless steel and AISI 304 austenitic stainless steel.

	Weight (%) Composition							
Materials	Fe	C	Si	Mn	P	S	Cr	Ni
AISI 430	Balance	0.055	0.045	0.420	0.031	0.008	17.0	–
AISI 304	Balance	0.08	1.00	2.00	0.045	0.03	20.0	10.0

TABLE 2. Mechanical properties of AISI 430 ferritic stainless steel and AISI 304 austenitic stainless steel.

Materials	Tensile Strength, MPa	Yield Strength 0.2% (MPa)	Elongation, %	Microhardness (Rockwell B′)
AISI 430	527	316	30	170
AISI 304	590	295	55	130–180

TABLE 3. Physical properties of AISI 430 ferritic stainless steel and AISI 304 austenitic stainless steel: α—thermal expansion coefficient (20–800°C), λ—thermal conductivity (20°C), Ω—electrical resistance (20°C), E—elastic modulus (20°C).

Materials	α, 10^{-6}	λ, W/(m·°C)	Ω, nΩ·m	E, kN/mm^2
AISI 430	13	24	600	225
AISI 304	20	15	700	200

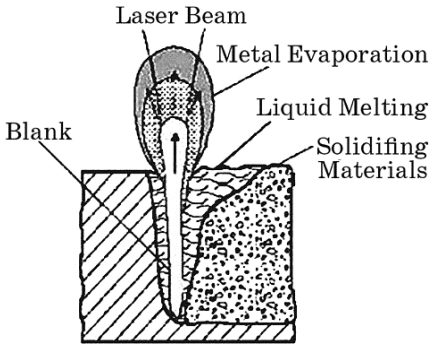

Fig. 1. Schematic illustration of LBW [20].

test piece. The laser welding experiments were carried under helium atmosphere with Trumpf Lazercell 1005 laser welding machine at 2000, 2250 and 2500 W heat inputs, 100 cm/min welding speed. Schematic illustration of LBW is given in Fig. 1 [20].

The Laser Beam Welding was carried out under helium atmosphere, 2000, 2250 and 2500 W different heat inputs and 100 cm/min constant welding speed. The welded specimens were cut perpendicularly to the welding zone for post evaluations of weld integrity. After the process, the samples were ground to an 80–1200-grit and etched by polishing them with 0.3 μm Al_2O_3 diamond paste and aqua region, respectively. For microstructural examination, AISI 430 material was etched electrolytically in a solution of 30% HCl + 10% HNO_3 + 30% H_2O solution and AISI 304 material was etched electrolytically in a solution of 50% HNO_3 + 50% H_2O solution. Then, the microstructures of welds were studied by means of scanning electron microscopy (SEM) equipped with energy depressive spectrometer (EDS). XRD analysis was performed to identify the structural phases.

Bending fatigue tests were conducted using a sinusoidal load of frequency 50 Hz and load ratio $R = -1$, at room temperature, considering as fatigue strength (Fig. 2). Six groups of fatigue specimens were prepared to obtain S–N curves. The welded interface was then cut longitudinally for investigation of the structural properties (Fig. 3). Fractography was also employed in evaluation of the fractured fatigue specimens.

3. RESULTS AND DISCUSSIONS

3.1. Microstructure

SEM images of welded joints under helium atmosphere at 2000, 2250 and 2500 W heat inputs and at 100 cm/min constant welding speeds

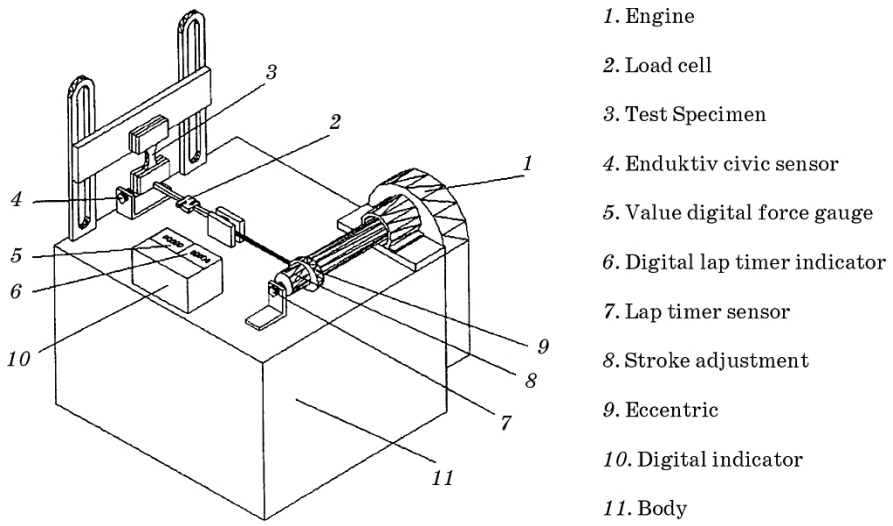

Fig. 2. Schematic illustration of fatigue test apparatus [34].

are presented in Figs. 4, *a*–*c*, respectively. Grain coarsening was observed at HAZ at both sides of weld interface and fine cracks were no traced at AISI 430 ferritic stainless and AISI 304 austenitic stainless steel side. Naturally, the area of weld (width) and heat-affected zone have increased at increased powers because of high heat input at weld seam. Similar results were achieved at the research of Karaaslan *et al.* and König *et al.* [31, 36].

It was determined that in the joint of AISI 430 ferritic stainless and AISI 304 austenitic stainless steel samples with laser beam welding at 2500W welding power, at 100 cm/min welding speed, and under helium shielding gas atmospheres, the penetration was completed and blanks or porosities in the weld were not observed. A homogeneous dispersion with small grains beginning from the zone with coarse grains on both sides appropriate for the original structure of the materials was also observed. Grain coarsening was observed at HAZ at both sides

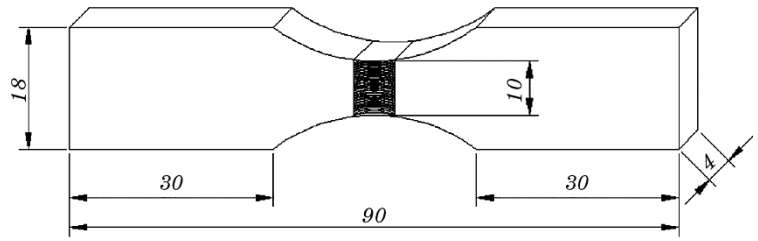

Fig. 3. Shape and measurement of the fatigue test specimens [35].

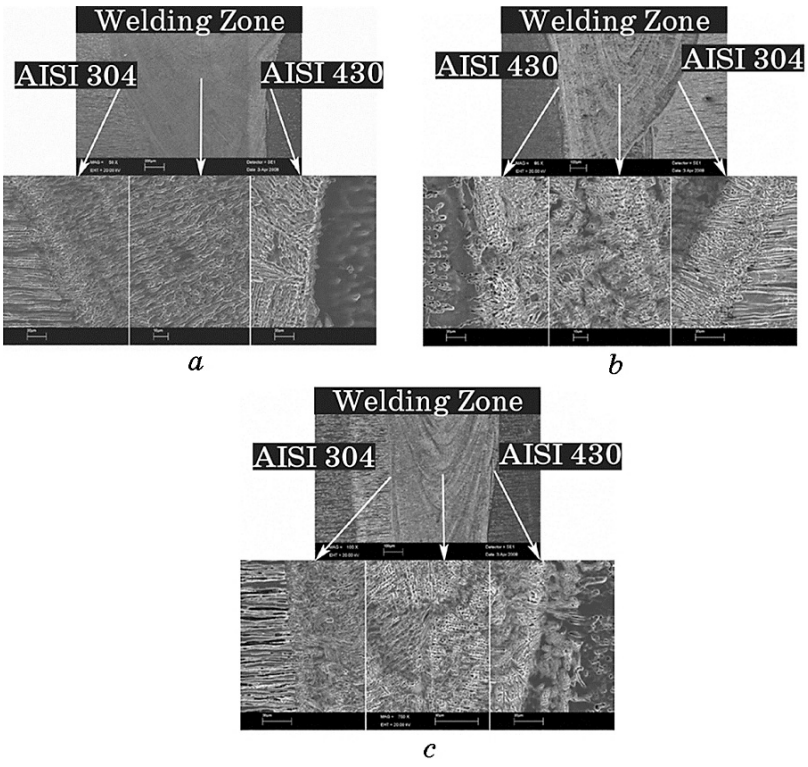

Fig. 4. SEM images of welded samples joined at heat input: 2000 W (*a*), 2250 W (*b*), and 2500 W (*c*).

of weld interface at AISI 430 ferritic and AISI 304 austenitic stainless steels side at ≅ 200–300 μm distances. In general, coefficient of thermal expansion of austenitic stainless steel is higher than that of ferritic stainless steel. Therefore, on both sides of the welding seam, there was no a specific grain hypertrophy, deformation and crack formation on the main materials. The SEM photographs indicate that microstructural features are affected significantly by welding power. The best properties were observed at the specimens welded at 2500 W heat input and at 100 cm/min welding speed.

3.2. Fatigue Test

Fatigue fractures, plastic deformation, tensile stress and fatigue cycled stresses also occur by the action. Therefore, as to avoid the occurrence of these three factors, fatigue cracks will not occur. Under a given applied stress amplitude cycles, the initiation of cracks in the material deformation and the tensile stress occurring in intermittent

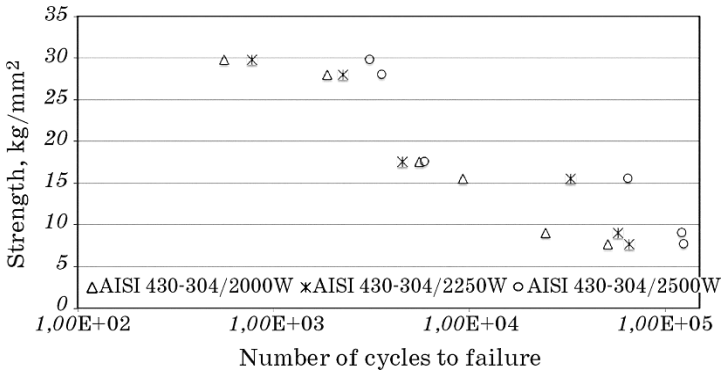

Fig. 5. Fatigue test results for welded joints.

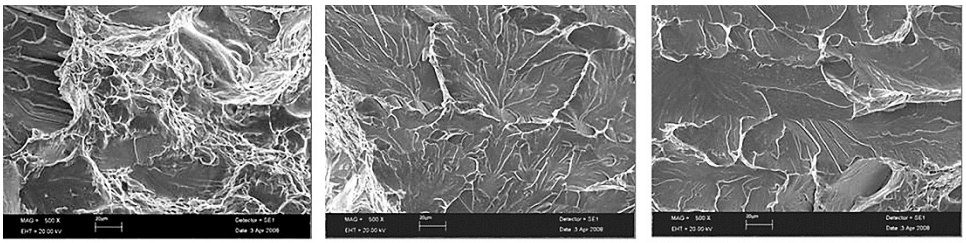

a *b* *c*

Fig. 6. Micrographs of the fatigue fracture surfaces of the specimens observed by SEM: 2000 W (*a*), 2250 W (*b*), 2500 W (*c*).

treatment is effective in the progression of cracks. Therefore, one of the main factors affecting fatigue mechanism is plastic deformation. Figure 5 shows fatigue test results for laser beam welded joints. According to the fatigue test results, the fatigue endurance increased with increasing the welding power. AISI 430–304/2500W joint exhibited better fatigue data from other welded joint types. Fatigue test was conducted under yield stresses.

3.3. Fractography

Plastic deformation detected in the specimens after the welding was not observed. This behaviour can also be seen in the micrographs of the fractured surfaces (Figs. 6, *a*–*c*). At fatigue strength tests, fractures were observed at AISI 430 side close to interface. After welding, it is seen that fatigue endurance can be increased with increasing the welding power, mainly in brittle fracture manner because AISI 430 steel is a brittle steel (Figs. 6, *a*–*c*). Under given conditions (2000, 2250 and 2500 W heat inputs, 100 cm/min welding speed) fatigue strengths

were close to parent material, and slightly increased at increased welding powers.

This can be explained with the increased heat input. The diffusion of carbon to AISI 430 side causes to the formation of chromium carbide precipitation at the grain boundaries, which are known to be deleterious to the fatigue life of material. The carbides at the grain boundaries provide preferential sites for cavity nucleation in ferritic stainless steels under fatigue conditions, thereby reducing the fatigue life [5, 20].

3.4. EDS Analysis

In the EDS analysis, in the 200 μm distance, from AISI 304 austenitic stainless steel to AISI 430 ferritic stainless steel 16% Chromium, 1.5% Carbon and 1% Nickel diffusion, the equal distance occurred from AISI 430 steel to AISI 304 steel chromium and carbon diffusion. As carbon is an interstitial element, stainless steel side will diffuse more easily. It is seen that chromium–nickel diffusion can be decreased by decreasing the welding power (Fig. 7).

In the XRD analysis, like Fe, Ni–Cr–Fe, Fe–Cr–Co–Ni–Mo–W and $Cr_2Fe_{6.7}Mo_{0.1}Ni_{1.3}Si_{0.3}$ phases were determined (Fig. 8). Intermetallic phase like $Cr_{23}C_6$ (chromium carbur), δ-ferrite and sigma were not observed.

4. CONCLUSIONS

In this study, the fatigue strength of AISI 430–304 stainless steels welded by CO_2 laser beam welding was investigated. The following results were obtained.

– AISI 430 ferritic stainless steel can be joined with AISI 304 austenitic stainless steel by laser welding process using helium atmosphere, at 2000, 2250 and 2500 W heat inputs, and 100 cm/min constant welding speed.

– At fatigue tests, fractures were observed close to AISI 430 side. After welding, it was seen that fatigue endurance decreased due to the decreasing of the welding power. This is caused by the fact that AISI 430 is brittle steel. However, fatigue endurance increased due to the increasing the heat input.

– The fatigue strength increases due to higher deep penetration with increasing welding power. The best properties were observed at the specimens welded at 2500 W heat input and at 100 cm/min welding speed.

– It was determined that the fusion zone was on average ≅ 1000–1800 μm in width, the deep penetration was on average ≅ 1300–2000

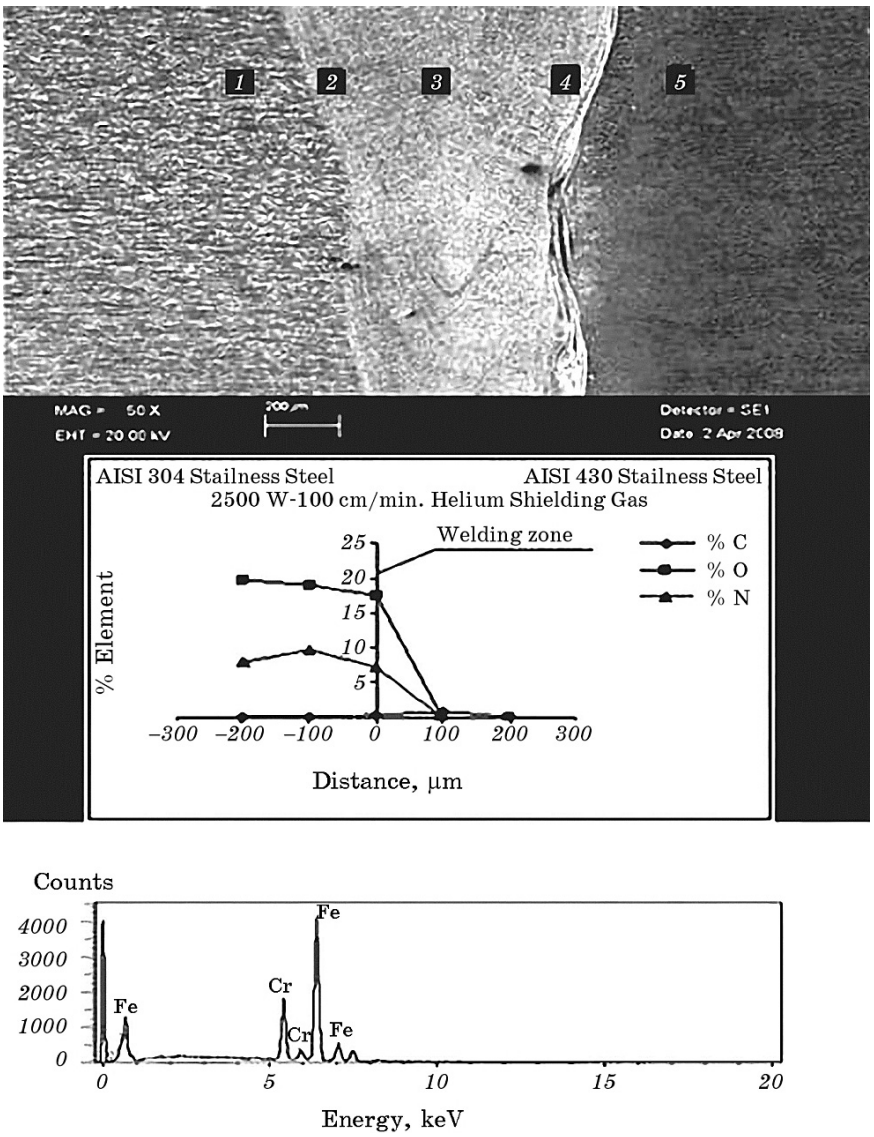

Fig. 7. EDS Analysis of AISI 430/304 (2500–100) sample.

μm in depth.

– Coefficient of thermal expansion of austenitic stainless steel is higher than that of ferritic stainless steel. Therefore, on both sides of the welding seam, there was no specific grain hypertrophy, deformation and crack formation on the main materials. The best properties in terms of microstructure were observed at the specimen bonded at 2500 W heat input, at 100 cm/min. welding speed and helium shield-

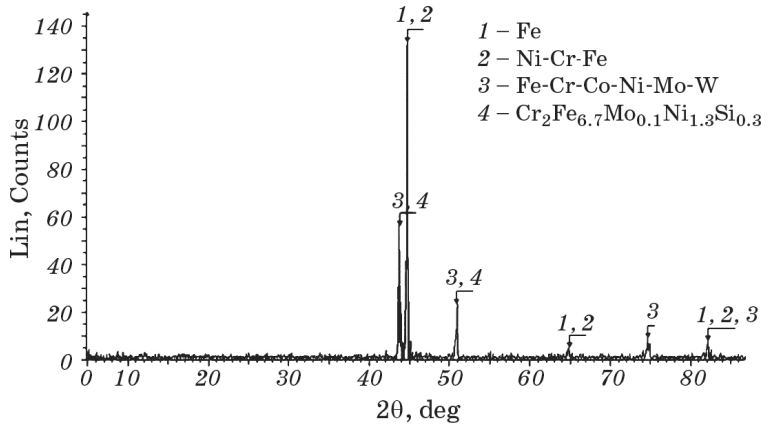

Fig. 8. XRD Analysis of AISI 430/304 (2500–100–Helium) sample.

ing gas.

– In the EDS analysis, in the 200 μm distance from AISI 304 austenitic stainless steel to AISI 430 ferritic stainless steel 16% chromium, 1.5% carbon and 1% Nickel diffusion, the equal distance occurred from AISI 430 steel to AISI 304 steel chromium and carbon diffusion. As carbon is an interstitial element, stainless steel side will diffuse more easily. It is seen that chromium–nickel diffusion can be decreased by decreasing the welding power.

– In the XRD analysis, like Fe, Ni–Cr–Fe, Fe–Cr–Co–Ni–Mo–W, and $Cr_2Fe_{6.7}Mo_{0.1}Ni_{1.3}Si_{0.3}$ phases were determined (Fig. 8). Intermetallic phase like $Cr_{23}C_6$ (chromium carbur), δ-ferrite and sigma were not observed.

ACKNOWLEDGEMENTS

The research was supported by the Scientific and Technological Research Council of Turkey (Project No: TUBITAK-108M401 and FUBAP: 1566).

REFERENCES

1. L. Yi-Chun and Y. Ming-Huei, *J. Mater. Process. Technol.*, **190**: 102 (2007).
2. M. Taskin, S. Ozan, and S. Kolukisa, *Practical Metallography*, **43**: 293 (2006).
3. S. Ozan, M. Taskin, and S. Kolukisa, *Practical Metallography*, **43**: 575 (2006).
4. A. Hascalik, E. Unal, and N. Ozdemir, *J. Mater. Sci.*, **41**: 3233 (2006).
5. U. Caligulu, H. Dikbas, and M. Taskin, *Gazi University J. Sci.*, **25**: 35 (2012).
6. P. Hussain and A. Isnin, *J. Mater. Process. Technol.*, **113**: 222 (2001).
7. C.-C. Hsieh, D.-Y. Lin, M.-C. Chen, and W. Wu, *Mater. Sci. Eng. A*, **477**: 328 (2008).

8. W. Ertle and R. J. Rockwell, *The Fabricator* (May 15, 2001).
9. B. S. Yilbas, M. Sami, J. Nickel, A. Coban, and S. A. M. Said, *J. Mater. Process. Technol.*, **82**: 13 (1998).
10. B. S. Yilbas, S. Z. Shuja, A. Arif, and M.A. Gondal, *J. Mater. Process. Technol.*, **135**: 6 (2003).
11. B. S. Yilbas, *J. Mater. Process. Technol.*, **70**: 264 (1997).
12. E. Bayraktar, D. Kaplan, and B. S. Yilbas, *J. Mater. Process. Technol.*, **204**: 440 (2008).
13. H. Guo Ming, Z. Jian, and L. Jian Qang, *Mater. Design*, **28**: 240 (2007).
14. K. Y. Benyounis, A. G. Olabi, and M. S. J. Hashmi, *J. Mater. Process. Technol.*, **164–165**: 978 (2005).
15. Y. Cui and C. D. Lundin, *Mater. Letters*, **59**: 2942 (2005).
16. M. Vural and A. Akkus, *J. Mater. Process. Technol.*, **153–154**: 1 (2004).
17. S. Y. Sirin, K. Sirin, and E. Kaluc, *Mater. Characterization*, **59**: 351 (2008).
18. L. W. Tsay, M. C. Young, and C. Chen, *Corrosion Sci.*, **45**: 1985 (2003).
19. A.-M. El-Batahgy, *Mater. Letters*, **32**: 155 (1997).
20. M. Taskin, U. Caligulu, and S. Kolukisa, *Practical Metallography*, **46**: 598 (2009).
21. U. Caligulu, M. Taskin, H. Dikbas, and A. K. Gur, *1st Intern. Conference on Welding Technologies (June 11–13, 2009)* (Ankara: Gazi University: 2009), p. 674.
22. F. Curcio, G. Daurelio, F. M. C. Minutolo, and F. Caiazzo, *J. Mater. Process. Technol.*, **175**: 83 (2006).
23. A. Zambon, P. Ferro, and F. Bonollo, *Mater. Sci. Eng. A*, **424**: 117 (2006).
24. P. Bertrand, I. Smurov, and G. Grevey, *Appl. Surf. Sci.*, No. 168 (2000).
25. A.-M. El-Batahgy, *Mater. Lett.*, **32**: 155 (1997).
26. F. M. Ghaini, M. J. Hamedi, M. J. Torkamany, and J. Sabbaghzadeh, *Scr. Mater.*, **56**: 955 (2007).
27. M. Vural, A. Akkus, and B. Eryurek, *J. Mater. Process. Technol.*, **176**: 127 (2006).
28. T. Yuri, T. Ogata, M. Saito, and Y. Hirayama, *Cryogenics*, **41**: 475 (2001).
29. C. Jang, P.-Y. Cho, M. Kim, S.-J. Oh, and J.-S. Yang, *Mater. Design*, **31**: 1862 (2010).
30. E. Taban, E. Deleu, A. Dhooge, and E. Kaluc, *Mater. Design*, **30**: 1193 (2009).
31. A. Karaaslan, N. Sonmez, and A. Topuz, *2nd Intern. Welding Technol. Conference (June, 1998, Istanbul, Turkey)* (in Turkish).
32. M. Sahin, *Mater. Design*, **28**: 2244 (2007).
33. M. Sahin and H. E. Akata, *Indust. Lubricate Tribol.*, No. 56: 2 (2004).
34. A. Sik, *Fatigue Test Machine*, Patent 2008/04670 (Gazi University, Faculty of Architecture, Department of Industrial Design, Ankara, Turkey: 2008) (in Turkish).
35. E. S. Kayali, C. Ensari, and F. Dikec, *Metalik Malzemelerin Mekanik Deneyleri* (ITU Library: 1983) (in Turkish).
36. R. Konig and N. Otmanboluk, *2nd Intern. Welding Technol. Conference (June, 1998, Istanbul, Turkey)*.